

Article

Mixed-Habit Type Ib-IaA Diamond from an Udachnaya Eclogite

Dmitry Zedgenizov ^{1,2,*}, Irina Bogush ³, Vladislav Shatsky ^{1,2}, Oleg Kovalchuk ³, Alexey Ragozin ^{1,2} and Viktoriya Kalinina ¹

¹ V.S. Sobolev Institute of Geology and Mineralogy, Siberian Branch of Russian Academy of Science, 630090 Novosibirsk, Russia; shatsky@igm.nsc.ru (V.S.); ragoz@igm.nsc.ru (A.R.); vika@igm.nsc.ru (V.K.)

² Geology and Geophysics Department, Novosibirsk State University, 630090 Novosibirsk, Russia

³ NIGP (Geo-Scientific research Enterprise) ALROSA Co., Chernyshevskoe rd. 7, 678170 Mirny, Sakha Republic, Russia; BogushIN@alrosa.ru (I.B.); KovalchukOE@alrosa.ru (O.K.)

* Correspondence: zed@igm.nsc.ru

Received: 13 October 2019; Accepted: 27 November 2019; Published: 29 November 2019



Abstract: The variety of morphology and properties of natural diamonds reflects variations in the conditions of their formation in different mantle environments. This study presents new data on the distribution of impurity centers in diamond type Ib-IaA from xenolith of biminerall eclogite from the Udachnaya kimberlite pipe. The high content of non-aggregated nitrogen C defects in the studied diamonds indicates their formation shortly before the stage of transportation to the surface by the kimberlite melt. The observed sectorial heterogeneity of the distribution of C- and A-defects indicates that aggregation of nitrogen in the octahedral sectors occurs faster than in the cuboid sectors.

Keywords: diamond; eclogite; nitrogen; mantle

1. Introduction

Diverse physical and chemical properties of natural diamonds are believed to reflect the variations in the conditions of their formation in contrasting media. It was established that in the lithospheric upper mantle the host to most diamonds are ultrabasic (peridotitic—P-type) and basic (eclogitic—E-type) rocks, which are often found as xenoliths in kimberlites [1]. Despite the majority of mineral inclusions in diamonds belong to peridotitic paragenesis [2,3] the most common diamondiferous xenoliths in kimberlites are eclogites [4]. Such diamondiferous xenoliths give unique opportunity for reconstruction of diamond-forming processes and allow identifying specific characteristics of diamonds in chemically different substrates.

It is suggested that eclogites can make up about 7% of the mass of the lithospheric upper mantle [5]. One of the dominant modern viewpoints on the origin of mantle eclogites is the formation in the process of subduction of the oceanic crust under ancient cratons [6–8]. Diamonds from mantle eclogites exhibit a diversity of morphological and color characteristics: octahedral crystals, macles, cuboids, and coated diamonds have been found in xenoliths of eclogites [9–14]. Eclogitic diamonds worldwide have wide variations of carbon isotope composition [15–17].

Most natural diamonds contain up to 3500 ppm of nitrogen as the primary structural impurity [18]. Nitrogen can produce a number of defects causing specific IR absorption, which allows to determine the type and content of each of these defects [19]. Other IR active structural defects in natural diamonds are related to hydrogen [20]. The majority of diamonds belong to the spectral type Ia and contain nitrogen atoms in forms of A-defects (the pair of nitrogen atoms replacing carbon at neighboring positions) or/and B-defects (the group of four carbon-substituting nitrogen atoms around vacancy). Diamonds of type Ib, where nitrogen is mainly presented as C-defects (single substitutional atoms) are

rare. The C center is responsible for the yellow/orange coloration of diamonds. The aggregation of C into A centers is well established experimentally as a result of extended heat treatments [21] and can be used as an indicator of thermal history of diamonds within the mantle [22]. In this work, we present new data on the distribution of nitrogen and hydrogen defects in type Ib-IaA diamond from xenolith of eclogite Ud-208-02 from Udachnaya kimberlite pipe.

2. Samples and Methods

The Udachnaya kimberlite pipe located in the central part of the Siberian craton (Figure A1) is a well-known locality that is a source of mantle xenoliths. Depleted granular garnet lherzolites and harzburgites form the principal rock type in the mantle of this region [23]. These rocks are common at the depth range corresponding to pressures 2.0–6.2 GPa. Deformed garnet lherzolites which are common in Udachnaya are believed to originate from secondary enrichment of depleted granular rocks by penetrating asthenospheric melts [24]. The temperatures of their formation are always higher compared to depleted rocks, indicating increased heat flow at the boundary between cratonic lithospheric mantle (CLM) and asthenosphere. The xenoliths of eclogites represent remnants of ancient (Archean) oceanic crust buried at the base of lithosphere after subduction [8].

The xenolith of bimineralic eclogite Ud-208-02 was found in kimberlite of Udachnaya pipe. The xenolith consists of xenomorphic grains (2–5 mm) of clinopyroxene (Cpx, 40% of the volume) and subhedral grains (3–8 mm) of garnet (Grt, 60% of the volume) (Figure 1). Some primary clinopyroxenes have experienced a significant secondary alteration. Accessory rutile grains (300–500 μm) are sometimes observed at the Cpx–Grt interfaces. The secondary veins and melt pockets consisting of altered glass and its replacement products evidence for partial melting of the xenolith [25]. Diamonds are located inside these veins and pockets. The compositions of rock-forming minerals (Table A1) have been analyzed using JEOL JXA-8100 electron probe micro-analyzer at the Analytical Center for Multi-elemental and Isotope Research SB RAS, Novosibirsk. The quantitative analyses were performed at 15 kV accelerating voltage, 20 nA sample current, and 2 μm beam diameter. The major components of garnet are almandine 46%, pyrope 29% and grossular 21%. Primary clinopyroxene is represented by omphacite (5.39 wt. % of Na_2O). The major elements in garnets and clinopyroxenes correspond to group B eclogites (Figure 2) [26,27], which are most common among eclogite xenoliths from Udachnaya kimberlites [28]. The calculated equilibrium temperature of clinopyroxene and garnet [29] in eclogite Ud-208-02 is 1130 $^{\circ}\text{C}$ (at $P = 5$ GPa). The pressure calculated at this temperature correspond to 8.2 GPa [30].

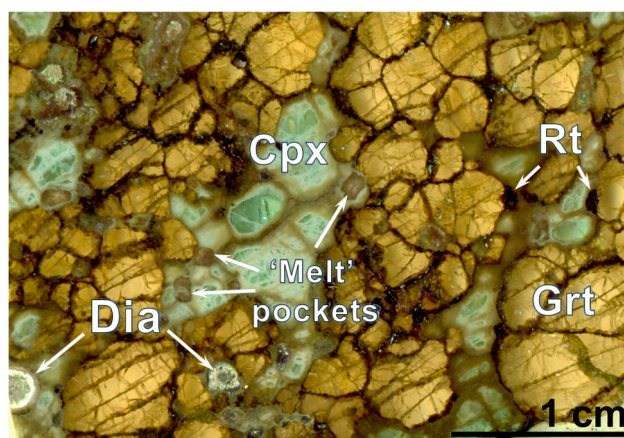


Figure 1. Petrographic features of eclogite Ud-208-02. Thin section showing euhedral grains of garnet (Grt), irregular grain boundaries of clinopyroxenes (Cpx), accessory rutiles (Rt), and diamonds (Dia). ‘Melt’ pockets are also shown.

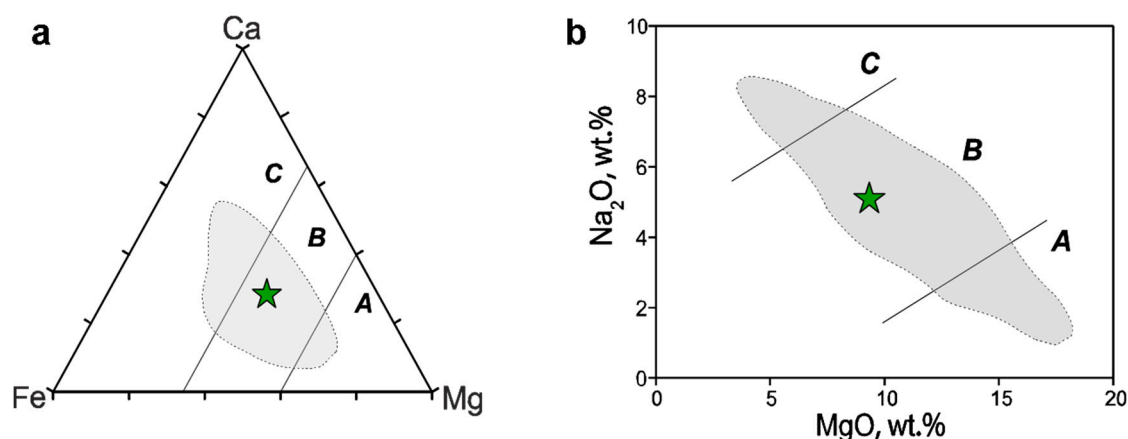


Figure 2. Compositional features of garnet (a) and clinopyroxene (b) from eclogite Ud-208-02, showing the three-fold (A, B, C) classification of eclogites, according to [26,27]. Garnet and clinopyroxene compositions from studied xenolith are shown as green star. The grey area represent the compositional ranges of garnets and clinopyroxenes from Udachnaya eclogites [4].

Eleven small diamond crystals (0.5–0.8 mm) were extracted after caustic fusion and acid dissolution of a part of xenolith. The crystals have bright yellow color caused by the presence of nitrogen C-centers detected by FTIR spectroscopy. The morphology of these diamonds were examined by optical (Zeiss Stemi 506 stereomicroscope) and scanning electron microscopy (SEM—scanning electron microscope HITACHI TM-1000) in regime of secondary electrons with an accelerating voltage of 15 kV and working distance of 15 mm. The morphology represent the curved shape of a cubic habit with concave surfaces (Figure 3). The carbon isotope composition of several diamonds have been determined using conventional mass-spectrometry following experimental procedure described in [31]. The $\delta^{13}\text{C}$ values of these diamonds vary in the range from -7.2 to -6.3‰ (Table A2) which closely corresponds to the average mantle values [32].

To characterize the internal structure and spectroscopic analysis, a double-side polished plate with a thickness of 200 μm oriented in the $\{110\}$ plane was prepared from the largest found crystal (Figure 4). The zonal and sectorial heterogeneity of color is observed in the crystal. The outer part of the crystal has a more saturated yellow color. Narrow colorless growth sectors $\{111\}$, developing in the direction of the vertices of the crystal, are clearly visible. Birefringence show strain pattern with higher interference between cuboid growth sectors. The birefringence in mixed-habit diamonds may be due to the variations in the lattice parameters caused by different concentrations of nitrogen defects between the octahedral and cuboid sectors [33]. Moreover, specific disc-crack-like defects in the cuboid sectors can also create their own localized strain fields and therefore produce birefringence [34].

To determine the distribution of nitrogen and hydrogen centers in the crystal, the plate was mapped using the FTIR spectroscopy. Local spectra ($50 \times 50 \mu\text{m}$) were recorded with a step of 50 μm and a resolution of 1 cm^{-1} on a Bruker VERTEX-70 Fourier spectrometer with a Hyperion 2000 microscope in Geo-Scientific research Enterprise (NIGP) ALROSA Co. Each spectrum was normalized by absorption in the two-phonon region and deconvoluted into spectra of pure Ib and IaA diamonds. The concentration of nitrogen defects was calculated using the coefficients $16.5 \times k1282 \text{ cm}^{-1}$ for A, ppm [35] and $25 \times k1130 \text{ cm}^{-1}$ for C, ppm [36], where $k1282 \text{ cm}^{-1}$ and $k1130 \text{ cm}^{-1}$ are absorption coefficient determined from deconvolution. The whole dataset (see Supplementary Materials) is presented in Table S1. The distribution images of nitrogen and hydrogen defects were obtained using ArcMap9.3 software (ESRI, Redlands, USA) with standard settings for constructing contours with equal intervals.

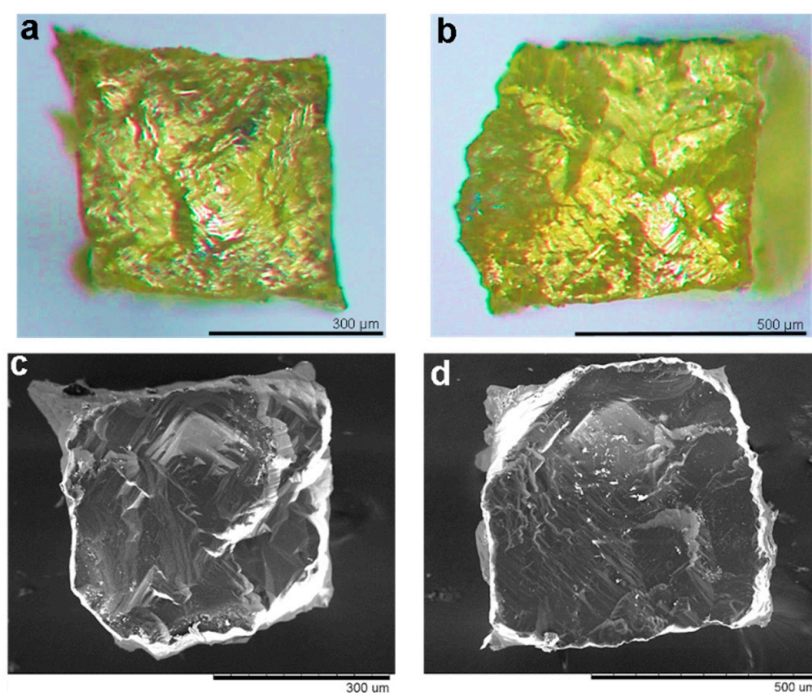


Figure 3. Morphology of diamonds from eclogite Ud-208-02: (a,b) microphotographs of yellow crystals with overall cubic habit; (c,d) SEM images of hopper cubic crystals.

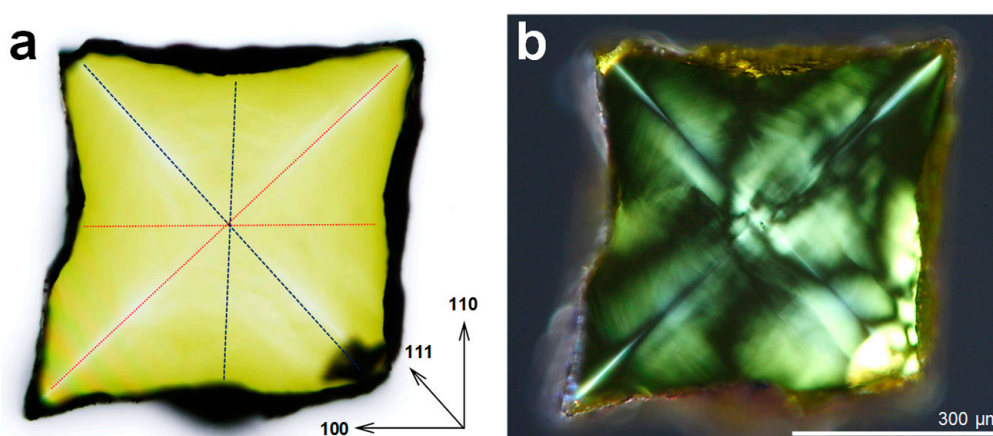


Figure 4. Polished plate of yellow cubic crystal showing colorless thin growth sectors {111}. (a) transmitted light, (b) birefringence pattern. Red lines on (a) are FTIR profiles on Figure 6a and dark blue lines are FTIR profiles on Figure 6b.

3. Results

All FTIR spectra from studied plate show the presence of nitrogen in the form of C- and A-defects (Figure 5). Content of these defects varies significantly from center to rim of the crystal and varies slightly in adjacent growth sectors of different growth zones (Figure 6). Total nitrogen content ($N = A + C$) is higher in central zone of the crystal (1350–1450 ppm), decreases (1200–1350 ppm) in intermediate zone and again increases (up to 1450 ppm) at the periphery. At that, content of A-defects decreases significantly from 988 ppm in the center to 443 ppm at the periphery of the crystal, whereas content of C-defects increases from 342 to 1011 ppm. Sectorial heterogeneity of the distribution of these defects is also observed, and it does not coincide with the zonal distribution over the total nitrogen content (Figure 7). Within the corresponding growth zones, content of C-defects is higher in cuboid sectors

than in octahedral ones whereas content of A-defects is lower. This distribution is also well manifested in the ratio of these two defects (nitrogen aggregation state $\%A = (A \times 100)/(C + A)$).

A narrow line at 3107 cm^{-1} suggesting the presence of hydrogen-related defects is fixed in FTIR spectra throughout the crystal. Intensity of this line ($\text{kH}_{3107\text{cm}}$) decreases from 2.2 cm^{-1} in the center to 0.7 cm^{-1} at the periphery of the crystal and does not correlate with the zonal and sectorial distribution of nitrogen defects (Figure 7). Based upon the most recent experimental data, it is thought that the defect giving rise to the 3107 cm^{-1} vibrational mode is vacancy-related and is likely to contain nitrogen [37].

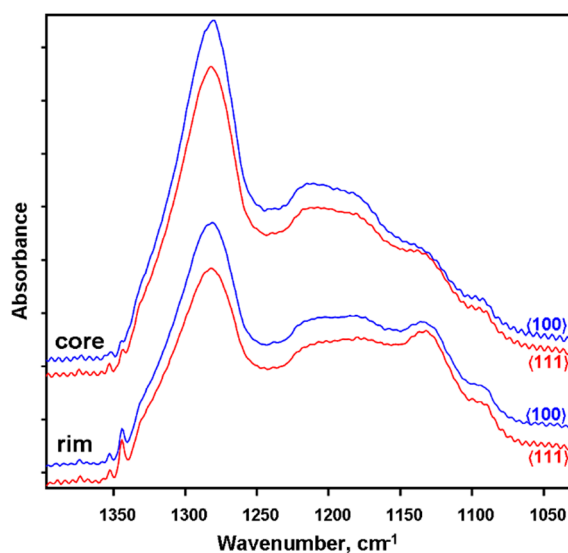


Figure 5. The FTIR spectra illustrating the absorption from structural nitrogen C- (band at 1130 cm^{-1} and line at 1344 cm^{-1}) and A-defects (band at 1282 cm^{-1}) in adjacent cubic {100} and octahedral {111} growth sectors in core and rim parts of the crystal from Figure 4.

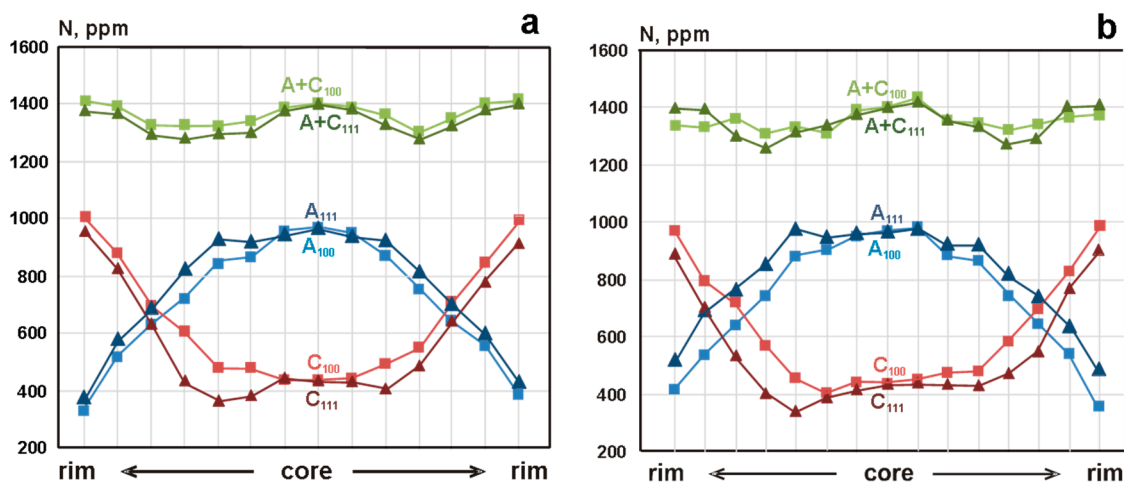


Figure 6. The profiles of nitrogen content (N, ppm) as C-defects, A-defects and their sum (A + C) in cubic {100} and octahedral {111} growth sectors throughout the crystal. (a,b) crossed profiles of adjacent sectors (see Figure 4).

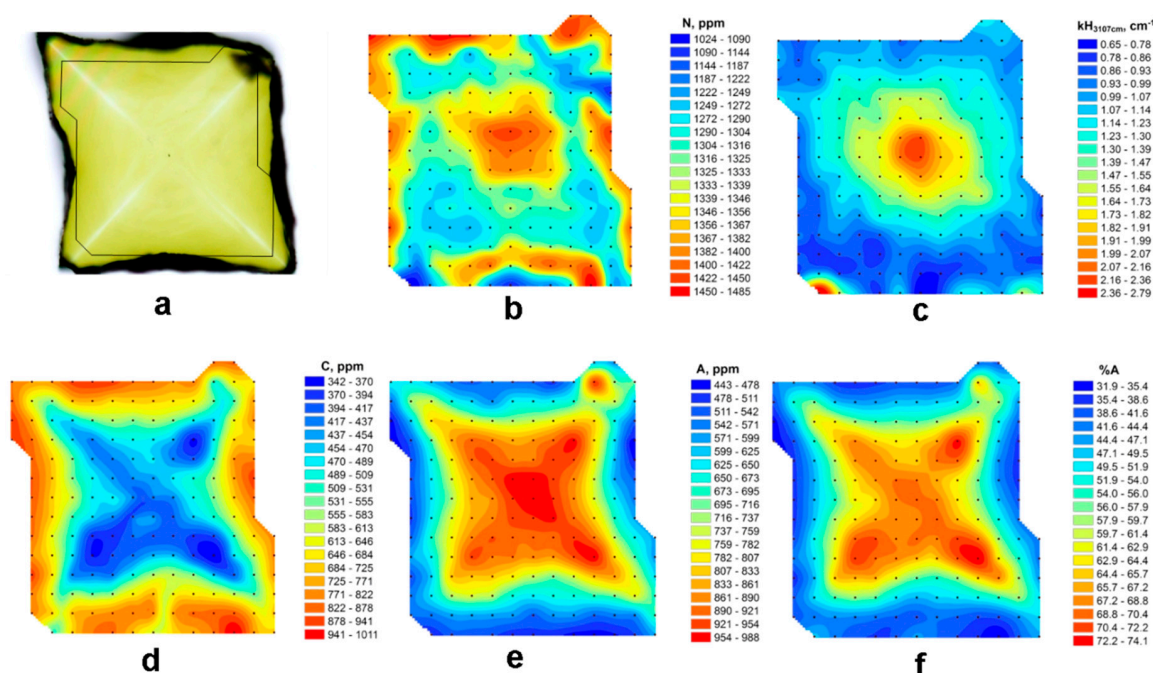


Figure 7. The distribution of nitrogen and hydrogen defects derived from quantitative FTIR mapping. (a) polished plate of diamond from eclogite Ud-208-02; (b) total nitrogen concentration (N, ppm); (c) the height of the 3107 cm^{-1} hydrogen-related band (kH_{3107} , cm^{-1}); (d) concentration of nitrogen as C-defects (C, ppm); (e) concentration of nitrogen as A-defects (A, ppm); (f) level of nitrogen aggregation (%A). Plots were produced using ArcMap 9.3 software.

4. Discussion

There are a lot of descriptions of xenolith of diamondiferous eclogites from the Udachnaya kimberlite pipe [8,13,25,28,38–41]. The chemical composition of diamondiferous eclogites does not differ from the composition of diamond-free eclogites, both in biminerals and other varieties. The compositions of primary clinopyroxene and garnet in studied eclogite correspond to that of Group B eclogites [26,27], which are most common in the Udachnaya kimberlite pipe. Only Group A from this classification were thought to be true mantle cumulates, whereas Groups B and C were considered as fragments of subducted oceanic crust [4]. Eclogites from Udachnaya represent oceanic crust of late Archean age, which was subducted and incorporated into a growing subcontinental lithosphere [42,43]. The variable oxygen isotope composition of mantle eclogites has been interpreted to represent the effects of both high- and low-temperature hydrothermal alterations of oceanic crust prior to subduction into the mantle [4,44,45]. These rocks have been stored in the mantle long period of Earth's history and finally returned to the surface by kimberlitic magmas 350–367 Ma ago [46,47].

The principal growth morphologies of natural diamonds are octahedral crystals with smooth faces and cuboids with kinked or rough surfaces but an overall cubic habit. It was assumed that the growth mechanisms are different for octahedral and cuboid diamonds [48]. The general model of diamond growth mechanisms and primary morphologies [49] is that at lower growth rates and driving forces, smooth growth occurs by the two-dimensional nucleation and dislocation/spiral growth mechanism, producing octahedral growth.

There are many descriptions of the morphology of natural diamonds of mixed habit when the simultaneous presence of flat faces of the octahedron and rough surfaces of the cuboid is observed. Such crystals are of great interest for determining the causes of variations in the properties of diamonds of different habit. The partitioning of nitrogen between octahedral and cuboid growth sectors was observed in some individual mixed-habit diamonds [50–53]. All diamonds in these studies belong to type IaAB, i.e., contained nitrogen in forms of aggregated A- and B-defects. In the present study, we

have described the diamond of type Ib-IaA, which is characterized by a zonal-sectorial distribution of nitrogen defects. Significant concentrations of non-aggregated nitrogen C-defects in the studied diamond indicate the formation of diamonds shortly before its transportation to the surface. However, Smit et al. [54] suggested that Ib diamonds from Zimmi (West Africa) after their formation were rapidly exhumed to shallower depths and then stored in cooler lithosphere for a long time.

The temperature and pressure of last equilibria of clinopyroxene and garnet in host eclogite Ud-208-02 is estimated at 1130 °C and 8.2 GPa respectively. Diamonds in this eclogite are located in suggested melt pockets filled with secondary minerals. Thus, the diamonds may be not syngenetic with the garnet and clinopyroxene in the host eclogite. This observation indicates metasomatic formation of diamonds at elevated temperatures, obviously post-dating the formation of their host eclogite [55]. Figure 8 displays the characteristics of nitrogen content and aggregation state in studied diamond in comparison with isochrons at temperatures 1130 °C and 1230 °C.

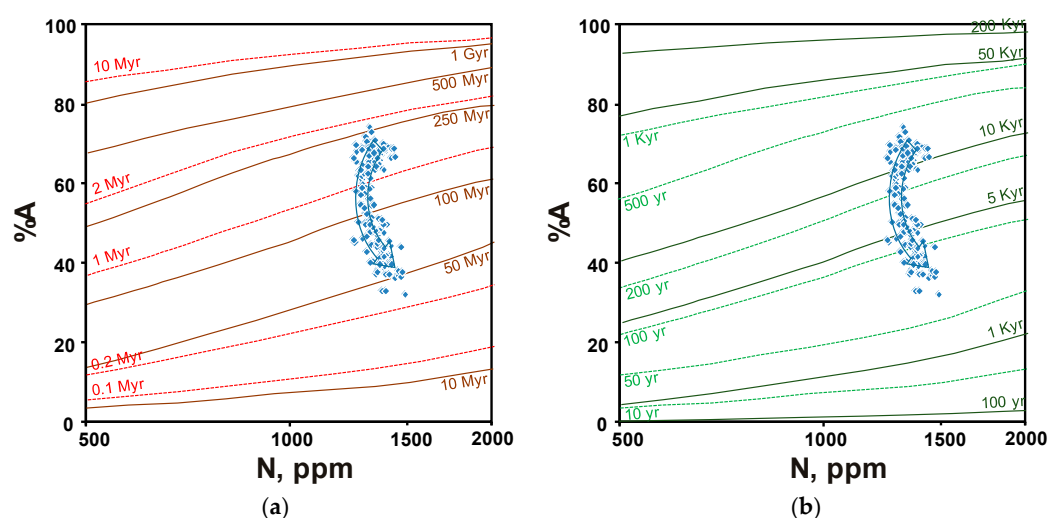


Figure 8. Nitrogen content plotted against the percentage of A aggregation ($\%A = (100 \times A)/(C + A)$) for diamond plate from Figure 4. Arrays show the core to rim variations. Isochrons for C defects (Type Ib) to A defects (Type IaA) aggregation for cubic (a) and octahedral (b) sectors were plotted from parameters given in [56] at $T = 1130$ °C (solid lines) and $T = 1230$ °C (dash line).

The zonal distribution of nitrogen observed in the crystal with an increasing of C-defects in the peripheral part agrees well with the ‘annealing’ model of A-defect formation [57]. At the same time, the observed sectorial heterogeneity of the distribution of these defects suggests that nitrogen aggregation in the octahedral sectors occurs faster than in the cuboid growth sectors. The significant difference in the activation energy of C- to A-defects aggregation for different growth sectors ($E_a = 6 \pm 0.2$ eV in cubic sectors and $E_a = 4.4 \pm 0.3$ eV in octahedral sectors) was previously recorded in natural and synthetic diamonds [46]. In addition, this artifact may be due to the fact that the transition of C- into A-defects for different forms of growth is described by different kinetic relationships. For example, it was shown that the order of kinetics may be different from second order [58]. Although the nitrogen aggregation mechanism is still under debate, the variations of rate constant are suggestive of an interstitial- or vacancy-assisted nitrogen aggregation mechanism [59]. The presence of vacancies along deformation lines may be the route along which aggregation proceeds [60]. However, we did not detect any signs of deformation in studied sample except strong strains in octahedral sectors, which can cause deformations. The lack of a relationship between the presence of a hydrogen defect and nitrogen content, which was detected in mixed-habit IaAB type diamonds [51], is probably associated either with a short residence time of the studied diamond or/and with a low annealing temperature, i.e., under conditions when aggregated B-defects do not form. The short mantle residence time of the mixed-habit Ib-IaA diamond, deduced from aggregation of C into A centers at temperatures of last

equilibration of host rock, indicates that diamond formation in mantle eclogites might be linked with not only ancient processes of subduction but with metasomatic event just prior to kimberlite eruption.

5. Conclusions

The findings of diamonds in mantle rocks preserved as xenoliths in kimberlites is important for reconstruction of diamond-forming processes. In this work, new data on the distribution of nitrogen and hydrogen defects in one of yellow cuboid diamonds found in eclogite Ud-208-02 from Udachnaya kimberlite pipe are presented. The formation of these diamonds is related to metasomatic event, obviously post-dating the formation of their host eclogite lastly equilibrated at temperature 1130 °C.

The polished plate made from one of the crystals reveals zonal and sectorial heterogeneity. It is detected that nitrogen presented only as C- and A-defects and its content varies significantly from center to rim and varies slightly in adjacent growth sectors of different growth zones. Hydrogen-related absorption at 3107 cm^{-1} does not correlate with the zonal and sectorial distribution of nitrogen defects. The rare among natural diamonds type Ib implying the presence of non-aggregated nitrogen C-defects suggest is probably associated either with a short residence time of the diamond or/and with a low annealing temperature, i.e., under conditions when aggregated B-defects do not form. Increasing of C-defects in the peripheral part of studied crystal agrees well with the ‘annealing’ model of A-defect formation. With the nitrogen aggregation mechanism, the observed sectorial heterogeneity suggests that nitrogen aggregation in the octahedral sectors occurs faster than in the cuboid ones.

Supplementary Materials: The following are available online at <http://www.mdpi.com/2075-163X/9/12/741/s1>.

Author Contributions: Conceptualization, D.Z. and V.S.; Methodology (FTIR) and software, I.B. and O.K.; Investigation (EMP), A.R.; Data curation, V.K.; Writing—original draft preparation, D.Z., Writing—review and editing, V.S., I.B., O.K., A.R., and V.K.

Funding: Work is done on state assignment of IGM SB RAS.

Conflicts of Interest: The authors declare no conflict of interest.

Appendix A

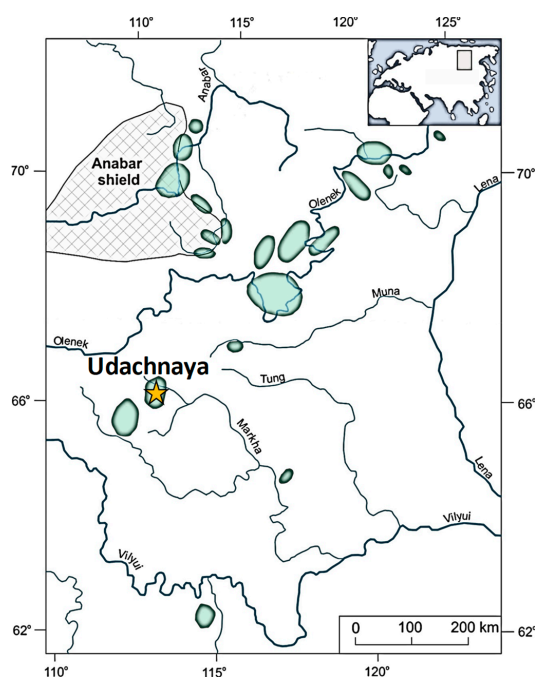


Figure A1. Location map of Udachnaya kimberlite pipe. The kimberlite fields of Siberian craton are shown as shaded area.

Table A1. Composition of rock-forming minerals of eclogite Ud-208-02.

	Cpx (n = 15)	σ	Grt (n = 16)	σ
wt. %				
SiO ₂	55.2	0.30	38.9	0.10
TiO ₂	0.16	0.02	0.15	0.02
Al ₂ O ₃	8.42	0.12	21.1	0.09
Cr ₂ O ₃	0.03	0.01	0.03	0.01
FeO	6.57	0.11	22.9	0.18
MnO	0.04	0.01	0.45	0.01
MgO	8.89	0.11	7.42	0.13
CaO	14.8	0.10	8.90	0.20
Na ₂ O	5.39	0.07	0.11	0.01
K ₂ O	0.06	0.00	-	-
Total	99.6	0.3	100.0	0.2
f.u.				
Si	1.998		2.999	
Ti	0.004		0.009	
Al	0.359		1.920	
Cr	0.001		0.002	
Fe	0.199		1.475	
Mn	0.001		0.030	
Mg	0.480		0.853	
Ca	0.576		0.737	
Na	0.379		0.016	
K	0.003		-	
Total	4.005		8.040	

Table A2. Carbon isotope composition of diamonds from eclogite Ud-208-02.

No.	Sample	$\delta^{13}\text{C}$, ‰
1	Ud-208-02 dia1	-6.7
2	Ud-208-02 dia2	-6.4
3	Ud-208-02 dia3	-7.2
4	Ud-208-02 dia5	-6.5
5	Ud-208-02 dia6	-6.3
6	Ud-208-02 dia8	-6.9
7	Ud-208-02 dia9	-7.1

References

1. Sobolev, N.V. *Deep-Seated Inclusions in Kimberlites and the Problem of the Composition of the Upper Mantle*; AGU: Washington, DC, USA, 1977; p. 279.
2. Efimova, E.S.; Sobolev, N.V. Abundance of crystalline inclusions in Yakutian diamonds. *Dokl. Akad. Nauk SSSR* **1977**, *237*, 1475–1478.
3. Stachel, T.; Harris, J.W. The origin of cratonic diamonds—Constraints from mineral inclusions. *Ore Geol. Rev.* **2008**, *34*, 5–32. [[CrossRef](#)]
4. Taylor, L.A.; Anand, M. Diamonds: Time capsules from Siberian mantle. *Geochemistry* **2004**, *64*, 1–74. [[CrossRef](#)]
5. Anderson, D.L. *Theory of the Earth*; Blackwell Scientific Publications: Boston, MA, USA, 1989.
6. Ringwood, A.E.; Green, D.H. An experimental investigation of the gabbro–eclogite transformation and some geophysical implications. *Tectonophysics* **1966**, *3*, 383–427. [[CrossRef](#)]
7. MacGregor, I.D.; Manton, W.I. Roberts Victor eclogites: Ancient oceanic crust. *J. Geophys. Res.* **1986**, *91*, 14063–14079. [[CrossRef](#)]
8. Jacob, D.; Jagoutz, E.; Lowry, D.; Matthey, D.; Kudrjavnitskaya, G. Diamondiferous eclogites from Siberia: Remnants of Archean oceanic crust. *Geochim. Cosmochim. Acta* **1994**, *58*, 5191–5207. [[CrossRef](#)]

9. Pokhilenko, N.P.; Sobolev, N.V.; Yefimova, Y.S. Xenolith of deformed diamond-bearing kyanite eclogite from the Udachnaya pipe, Yakutia. *Dokl. Akad. Nauk SSSR* **1982**, *266*, 212–216.
10. Spetsius, Z.V. Diamondiferous Eclogites from Yakutia: Evidence for a Late and Multistage Formation of Diamonds. In Proceedings of the 6th International Kimberlite Conference, Novosibirsk, Russia, 30 July–19 August 1995; pp. 572–574.
11. Harlow, G.E. *The Nature of Diamonds*; Cambridge University Press: Cambridge, UK, 1998.
12. Sobolev, N.V.; Taylor, L.A.; Zuev, V.M.; Bezborodov, S.M.; Snyder, G.A.; Sobolev, V.N.; Yefimova, E.S. The specific features of eclogitic paragenesis of diamonds from Mir and Udachnaya kimberlite pipes (Yakutia). *Russ. Geol. Geophys.* **1998**, *39*, 1653–1663.
13. Shatsky, V.S.; Zedgenizov, D.A.; Ragozin, A.L. Evidence for a subduction component in the diamond-bearing mantle of the Siberian craton. *Russ. Geol. Geophys.* **2016**, *57*, 111–126. [[CrossRef](#)]
14. Shatsky, V.S.; Ragozin, A.L.; Zedgenizov, D.A.; Mityukhin, S.I. Evidence for multistage evolution in a xenolith of diamond-bearing eclogite from the Udachnaya kimberlite pipe. *Lithos* **2008**, *105*, 289–300. [[CrossRef](#)]
15. Javoy, M.; Pineau, F.; Delorme, H. Carbon and nitrogen isotopes in the mantle. *Chem. Geol.* **1986**, *57*, 41–62. [[CrossRef](#)]
16. Shatsky, V.S.; Zedgenizov, D.A.; Ragozin, A.L.; Kalinina, V.V. Carbon isotopes and nitrogen contents in placer diamonds from the NE Siberian craton: Implications for diamond origins. *Eur. J. Mineral.* **2014**, *26*, 41–52. [[CrossRef](#)]
17. Galimov, E.M. Isotope fractionation related to kimberlite magmatism and diamond formation. *Geochim. Cosmochim. Acta* **1991**, *55*, 1697–1708. [[CrossRef](#)]
18. Cartigny, P. Stable isotopes and origin of diamond. *Elements* **2005**, *1*, 79–84. [[CrossRef](#)]
19. Zaitsev, A.M. *Optical Properties of Diamond: A Data Handbook*; Springer: Berlin/Heidelberg, Germany, 2001; p. 502.
20. De Weerd, F.; Pal'yanov, Y.N.; Collins, A.T. Absorption spectra of hydrogen in ¹³C diamond produced by high-pressure, high-temperature synthesis. *J. Phys. Condens. Matter* **2003**, *15*, 3163–3170. [[CrossRef](#)]
21. Evans, T.; Qi, Z.; Maguire, J. The stages of nitrogen aggregation in diamond. *J. Phys. C Solid State Phys.* **1981**, *14*, 379. [[CrossRef](#)]
22. Taylor, W.R.; Bulanova, G.; Milledge, H.J. Quantitative nitrogen aggregation study of some Yakutian diamonds: Constraints on the growth, thermal and deformation history of peridotitic and eclogitic diamonds. *Int. Kimberl. Conf. Ext. Abstr.* **1995**, *6*, 608–610.
23. Boyd, F.R.; Pokhilenko, N.P.; Pearson, D.G.; Mertzman, S.A.; Sobolev, N.V.; Finger, L.W. Composition of the Siberian cratonic mantle: Evidence from Udachnaya peridotite xenoliths. *Contrib. Mineral. Petrol.* **1997**, *128*, 228–246. [[CrossRef](#)]
24. Tyckov, N.S.; Agashev, A.M.; Malygina, E.V.; Nikolenko, E.I.; Pokhilenko, N.P. Thermal perturbations in the lithospheric mantle as evidenced from P–T equilibrium conditions of xenoliths from the Udachnaya kimberlite pipe. *Dokl. Earth Sci.* **2014**, *454*, 84–88. [[CrossRef](#)]
25. Misra, K.C.; Anand, M.; Taylor, L.A.; Sobolev, N.V. Multi-stage metasomatism of diamondiferous eclogite xenoliths from the Udachanay kimberlite pipe, Yakutia, Siberia. *Lithos* **2004**, *146*, 696–714.
26. Coleman, R.G.; Lee, D.E.; Brannock, W.W. Eclogites and eclogites, their difference and similarities. *Bull. Geol. Soc. Am.* **1965**, *76*, 483–508. [[CrossRef](#)]
27. Taylor, L.A.; Neal, C.R. Eclogites with oceanic crustal and mantle signature from Bellsbank kimberlite, South Africa, Part I: Mineralogy, petrography, and whole rock chemistry. *J. Geol.* **1989**, *97*, 551–567. [[CrossRef](#)]
28. Sobolev, V.N.; Taylor, L.A.; Snyder, G.A.; Sobolev, N.V. Diamondiferous eclogites from the Udachnaya kimberlite pipe, Yakutia. *Int. Geol. Rev.* **1994**, *36*, 42–64. [[CrossRef](#)]
29. Ellis, D.J.; Green, D.H. An experimental study of the effect of Ca upon garnet clinopyroxene Fe–Mg exchange equilibria. *Contrib. Mineral. Petrol.* **1979**, *71*, 13–22. [[CrossRef](#)]
30. Beyer, C.; Frost, D.J.; Miyajima, N. Experimental calibration of a garnet-clinopyroxene geobarometer for mantle eclogites. *Contrib. Mineral. Petrol.* **2015**, *169*, 18. [[CrossRef](#)]
31. Reutsky, V.N.; Borzdov, Y.M.; Palyanov, Y.N. Effect of diamond growth rate on carbon isotope fractionation in Fe–Ni–C system. *Diam. Relat. Mater.* **2012**, *21*, 7–10. [[CrossRef](#)]
32. Stachel, T.; Harris, J.W.; Muehlenbachs, K. Sources of carbon in inclusion bearing diamonds. *Lithos* **2009**, *112*, 625–637. [[CrossRef](#)]

33. Howell, D. Strain-induced birefringence in natural diamond: A review. *Eur. J. Mineral.* **2012**, *24*, 575–585. [[CrossRef](#)]
34. Walmsley, J.C.; Lang, A.R.; Rooney, M.-L.T.; Welbourn, C.M. Newly observed microscopic planar defects on {111} in natural diamond. *Philos. Mag. Lett.* **1987**, *55*, 209–213. [[CrossRef](#)]
35. Boyd, S.R.; Kiflawi, I.; Woods, G.S. The relationship between infrared absorption and the A defect concentration in diamond. *Philos. Mag. B* **1994**, *69*, 1149–1153. [[CrossRef](#)]
36. Kiflawi, I.A.; Mayer, E.; Spear, P.M.; Woods, G.S. Infrared absorption by the single nitrogen and A defect centres in diamond. *Philos. Mag. B* **1994**, *69*, 1141–1147. [[CrossRef](#)]
37. Goss, J.P.; Briddon, P.R.; Hill, V.; Jones, R.; Rayson, M.J. Identification of the structure of the 3107 cm⁻¹ H-related defect in diamond. *J. Phys. Condens. Matter* **2014**, *26*, 145801. [[CrossRef](#)] [[PubMed](#)]
38. Jerde, E.A.; Taylor, L.A.; Crozaz, G.; Sobolev, N.V.; Sobolev, V.N. Diamondiferous eclogites from Yakutia, Siberia: Evidence for a diversity of protoliths. *Contrib. Mineral. Petrol.* **1993**, *114*, 189–202. [[CrossRef](#)]
39. Snyder, G.A.; Jerde, E.A.; Taylor, L.A.; Halliday, A.N.; Sobolev, V.N.; Sobolev, N.V. Nd and Sr isotopes from diamondiferous eclogites, Udachnaya kimberlite pipe, Yakutia, Siberia: Evidence of differentiation in the early Earth? *Earth Planet. Sci. Lett.* **1993**, *118*, 91–100. [[CrossRef](#)]
40. Snyder, G.A.; Taylor, L.A.; Jerde, E.A.; Clayton, R.N.; Mayeda, T.K.; Deines, P.; Rossman, G.; Sobolev, N.V. Archean mantle heterogeneity and the origin of diamondiferous eclogites, Siberia: Evidence from stable isotopes and hydroxyl in garnet. *Am. Mineral.* **1995**, *80*, 799–809. [[CrossRef](#)]
41. Taylor, L.A.; Keller, R.A.; Snyder, A.; Wang, W.; Carlson, W.D.; Hauri, E.H.; McCandless, T.; Kim, K.; Sobolev, N.V.; Bezborodov, S.M. Diamonds and their mineral inclusions, and what they tell us: A detailed “Pull-Apart” of a diamondiferous eclogite. *Int. Geol. Rev.* **2000**, *42*, 959–983. [[CrossRef](#)]
42. Pearson, D.G.; Snyder, G.A.; Shirey, S.B.; Taylor, L.A.; Carlson, R.W.; Sobolev, N.V. Archean Re–Os age for Siberian eclogites and constraints on Archean tectonics. *Nature* **1995**, *374*, 711–713. [[CrossRef](#)]
43. Jacob, D.E.; Foley, S.F. Evidence for Archean ocean crust with low high field strength element signature from diamondiferous eclogite xenoliths. *Lithos* **1999**, *48*, 317–336. [[CrossRef](#)]
44. Jacob, D.E. Nature and origin of eclogite xenoliths from kimberlites. *Lithos* **2004**, *77*, 295–316. [[CrossRef](#)]
45. Ickert, R.B.; Stachel, T.; Stern, R.A.; Harris, J.W. Diamond from recycled crustal carbon documented by coupled $\delta^{18}\text{O}$ – $\delta^{13}\text{C}$ measurements of diamonds and their inclusions. *Earth Planet. Sci. Lett.* **2013**, *364*, 85–97. [[CrossRef](#)]
46. Davis, G.L.; Sobolev, N.V.; Kharkiv, A.D. New data on the age of Yakutian kimberlites obtained by the U–Pb method on zircons. *Dokl. Akad. Nauk SSSR* **1980**, *254*, 175–179.
47. Kinny, P.D.; Griffin, B.; Heaman, L.M.; Brakhfogel, F.F.; Spetsius, Z.V. SHRIMP U–Pb ages of perovskite from Yakutian kimberlites. *Russ. Geol. Geophys.* **1997**, *38*, 91–99.
48. Moore, M.; Lang, A.R. On the internal structure of natural diamonds of cubic habit. *Philos. Mag.* **1972**, *26*, 1313–1325. [[CrossRef](#)]
49. Sunagawa, I. Growth and morphology of diamond crystals under stable and metastable conditions. *J. Cryst. Growth* **1990**, *99*, 1156–1161. [[CrossRef](#)]
50. Zedgenizov, D.A.; Harte, B. Microscale variations of $\delta^{13}\text{C}$ and N content in diamonds with mixed-habit growth. *Chem. Geol.* **2004**, *205*, 169–175. [[CrossRef](#)]
51. Howell, D.; Griffin, W.L.; Piazzolo, S.; Say, J.M.; Stern, R.A.; Stachel, T.; Nasdala, L.; Rabeau, J.R.; Pearson, N.J.; O’Reilly, S.Y. A spectroscopic and carbon-isotope study of mixed-habit diamonds: Impurity characteristics and growth environment. *Am. Mineral.* **2013**, *98*, 66–77. [[CrossRef](#)]
52. Smit, K.V.; Shirey, S.B.; Stern, R.A.; Steele, A.; Wang, W. Diamond growth from C–H–N–O recycled fluids in the lithosphere: Evidence from CH₄ micro-inclusions and $\delta^{13}\text{C}$ – $\delta^{15}\text{N}$ –N content in Marange mixed-habit diamonds. *Lithos* **2016**, *265*, 68–81. [[CrossRef](#)]
53. Skuzovatov, S.Y.; Zedgenizov, D.A.; Rakevich, A.L. Spectroscopic constraints on growth of Siberian mixed-habit diamonds. *Contrib. Mineral. Petrol.* **2017**, *172*, 46. [[CrossRef](#)]
54. Smit, K.V.; Shirey, S.B.; Wang, W. Type Ib diamond formation and preservation in the West African lithospheric mantle: Re–Os age constraints from sulphide inclusions in Zimmi diamonds. *Precambrian Res.* **2016**, *286*, 152–166. [[CrossRef](#)]
55. Anand, M.; Taylor, L.A.; Misra, K.C.; Carlson, W.D.; Sobolev, N.V. Nature of diamonds in Yakutian eclogites: Views from eclogite tomography and mineral inclusions in diamonds. *Lithos* **2004**, *77*, 333–348. [[CrossRef](#)]

56. Taylor, W.R.; Canil, D.; Millendge, H.J. Kinetics of Ib to IaA nitrogen aggregation in diamond. *Geochim. Cosmochim. Acta* **1996**, *60*, 4725–4733. [[CrossRef](#)]
57. Evans, T. Changes produced by high temperature treatment of diamond. In *The properties of Diamond*; Evans, T., Field, J.E., Eds.; Academic Press: New York, NY, USA, 1979.
58. Stepanov, A.; Shatsky, V.; Zedgenizov, D.; Sobolev, N. Causes of variations in morphology and impurities of diamonds from the Udachnaya Pipe eclogite. *Russ. Geol. Geophys.* **2007**, *48*, 758–769. [[CrossRef](#)]
59. Collins, A.T. Vacancy enhanced aggregation of nitrogen in diamond. *J. Phys. C Solid State Phys.* **1980**, *13*, 2641. [[CrossRef](#)]
60. Smit, K.V.; D’Haenens-Johansson, U.F.S.; Howell, D.; Loudin, L.C.; Wang, W. Deformation-related spectroscopic features in natural Type Ib-IaA diamonds from Zimmi (West African craton). *Mineral. Petrol.* **2018**, *112*, 243–257. [[CrossRef](#)]



© 2019 by the authors. Licensee MDPI, Basel, Switzerland. This article is an open access article distributed under the terms and conditions of the Creative Commons Attribution (CC BY) license (<http://creativecommons.org/licenses/by/4.0/>).